

Experimental Verification of Cusp Heights when 3D Milling Rounded Surfaces

Balázs Mikó¹, Jozef Beňo², Ildikó Maňková²

¹Óbuda University Budapest, Donát Bánki Faculty of Mechanical and Safety Engineering, Népszínház u. 8, 1084 Budapest, Hungary
miko.balazs@bgk.uni-obuda.hu

²Technical University Košice, Faculty of Mechanical Engineering, Mäsiarska 74, 040 01 Košice, Slovakia, jozef.beno@tuke.sk, ildiko.mankova@tuke.sk

Abstract: The paper deals with the experimental verification of cusp height when finishing an elementary surface by end ball milling. The relationship expressing the effect of the direction of milling cutter motion on cusp heights has been derived from the geometrical interpretation of inclined elementary surface. Experimental verification has been carried out as 3D milling of surface with definite roundness while surface roughness was measured considering normal vectors of tool-workpiece contact. An approach based on process window has been used to evaluate the measured data.

Keywords: ball end milling; cusp height; roughness data; process window

1 Introduction

Tool making and mould production technology became a key aspect in product innovation because of wide scale application of design features based on formed and free-form surfaces. Software development, CAD and CAM products, programming and control of machine tools as well as advanced metal cutting tools represent main driving forces associated with mould making in various industrial sectors. The production of both formed and free-form surfaces by milling has replaced traditional technologies such as electro-discharge machining and electro-chemical machining, the latter being of high power consumption rate. This fact is a very influential factor and hence contributes to the reduction of product life cycles and an increasing innovation rate in machinery products [1].

Formed and free-form surfaces result from the required shape of the final engineering component in the design of tooling and molding, whereas the form of any surface is usually generated by means of CAD, and are subsequently transferred into the control unit of any CNC milling machine. According to the current state of the art, the scientific sources characterizing the field of formed surfaces may be classified into five main fields as follows:

- 1 Parametric and geometrical definition of any formed and free-form surface; formal expression, surface slicing, surface segmentation, etc.
- 2 Decomposition of any surface for the control unit of machine tool motion, and that is subject of programming of tool paths, which include the choice of metal removal strategy, the visual representation of metal removal by tool edge, etc.
- 3 Graphical and analytical expression of machined surface texture generated by the tool, machined surface inclination in terms of the normal vectors, surface generation due to tool motion, etc.
- 4 Modeling of material removal as well as establishing of various dependencies based either on one quantity or more; while cutting force components and tool wear represent the data widely discussed in scientific sources.
- 5 Time of machining of any formed surface, cutting conditions, the influence of cutting conditions on a machined surface, the resultant surface quality and its representation.

On the other hand, the tool edge of metal cutting tools (end milling cutter, end ball milling cutter for formed surface semi-finishing) are considered to be the factors of technology of removal, see in Fig. 1, while influences of tool edge shape/geometry on resultant surface quality of produced surfaces are discussed, e.g. in [2].

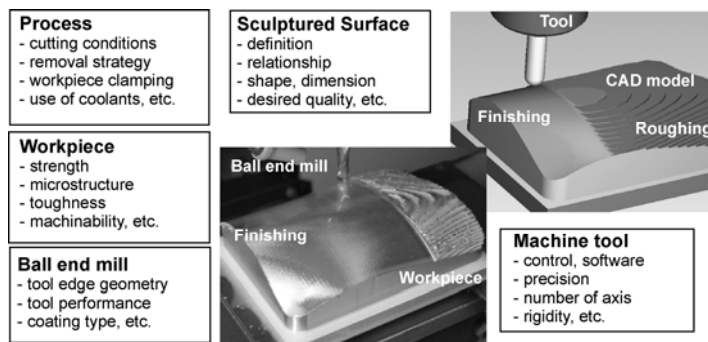


Figure 1

Factors affecting the quality of the product when machining with ball end milling

Based on the factors shown in Fig 1, the following notes are added to the machining of any free-form surface. First, commercial CAD/CAM systems provide various capabilities for surface design and process planning. Second, an efficient process plan requires the establishment of proper operation sequences, including removal strategies, that is, tooling and tool performance. In other words, no firm rules are available to enter any removal strategy for different manufacturability of designed free-form surface. Finally, yet more importantly, the economics of free-form machining imply as well the consideration of the tool performance, surface quality, and production costs.

2 Review of some Recent Results

The machined surface belongs to the most discussed subjects regarding product quality when milling by ball end mill cutters. Due to variability in technology such as cutting conditions, tool material/tool shape, milling strategy, etc., the resultant surface roughness varies widely by being affected by the type of produced surface and workpiece as well; see sources given in Tab. 1. Becze [4] showed that the roughness range varies due to the design of the die cavity, which differentiates it from straight surface, wall, and corner. As realized by [5], three common values of roughness exist which distinguishes the level of finishing, and the best of them, $Ra \approx 0.5 \mu\text{m}$ refers to equivalent of manual polishing. According to [6], there is no uniformity of roughness range because of the coating applied to end mill cutter. In general, the best surface quality ($Ra = 0.5 \div 0.8 \mu\text{m}$) results from milling with CBN tools. As found by [7], the resultant roughness depends on tool deflection. Because of very specific appearance of machined surface, the so called topomorphy was introduced by [8]. However, the outer topomorphy by [8] differs greatly between up milling and down milling. Roughness data by [8] from Table 1 characterizes the former and the latter.

Table 1
Some roughness data resulting from ball end milling

Source	Workpiece	Type of surface	Roughness [μm]
Gilles et al. [3]	C 35E steel	planar	$Ra = 0.90 - 1.26$
Becze et al. [4]	Steel 62 HRC	die cavity	$Ra = 0.22 - 1.22$
Baptista, Simoes [5]	Aluminum	convex, concave	$Ra = 0.29 - 3.10$
Fallböhmer et al. [6]	P20 steel	planar	$Ra = 0.80 - 5.00$
de Lacalle et al. [7]	Steel 62 HRC	complex form	$Ra = 1.47 - 2.79$
Antoniadis et al. [8]	C 60 steel	planar, oblique	$Rz = 1.00 - 4.00$

The next feature of surface quality during 3D milling is tolerance, often called the allowed errors of both dimension and shape. These tolerances determine the conditions when generating tool path, especially the tolerance for path interpolation and the tolerance of cusp height [9]. The generation of scallop height has been studied in [10] and its dimension varies within app $13.5 \div 2000 \mu\text{m}$ in 3D milling. Jerard et al. [11] pointed out that cutting simulation error is caused by deviation between the actual surface and the polyhedral approximation and protrusion of the tool between the surface points. When the polyhedral approximation lies inside the surface, the simulation error is the sum of the former and the latter. Finally, the resultant tolerance follows from ball end mill diameter and protrusion of the tool between the surface points. Narita et al. [12] showed that machining errors result from the deformation of the used milling tool. Similarly, Kim et al. [13] developed a method of surface error calculation based on beam deflection. Form errors from app zero to app 0.2 mm depend mainly on the inclination angle of machined surface, as the former (error app zero) refers to a

plain surface and the latter refers to inclination angle of 60 deg. Fallböhrer *et al.* [6] introduced average dimensional errors within $0.02 \div 0.06$ mm for injection moulds and stamping dies, respectively. Nevertheless, an improved surface finish can be achieved either through an increased number of finishing paths or with a larger diameter cutter. According to [6], cusp height (Ch) is identical with theoretical surface roughness R_{th} . De Lacalle *et al.* [7] introduced a new methodology for the selection of the tool paths on complex surfaces that minimize dimensional errors due to tool deflection in three axes milling. The methodology enabled dimensional errors to fall from 30 mm to below 4 mm in 3D milling. Dimensional errors, however, depend on the deflection force which is defined to be perpendicular to the tool axis and projected on the plane defined by the tool axis and the normal vector to the machined surface.

In addition to the factors associated with surface quality that have been discussed above (roughness, cusp/scallop height, tolerances and errors due to machining), there is another factor in the research of 3D milling of both formed and free-form surfaces, i.e. the design of the tested workpiece. There is no uniqueness in designing a tested workpiece as it varies in quite different shapes. A tested workpiece as a planar object gives results as tool axis orientation, transversal cutting force, tool vibrations, and surface roughness [3]. Planar surface of tested object enables us to use specific techniques such as an inclined slot cutting test [13]. The combination of two such surfaces as convex and/or concave denotes another possibility to combine milling of part of any free form surface, for instance [10], or machined surface enables us to apply so called wavelet-based multi-resolution representation of a series of intermediate shape models according to [14]. The inclined planar surface gained wide applicability in 3D milling; however, the inclination angle of a planar surface is very manageable for copying a very small portion of free form surface. The inclination angle of a planar surface can be equal to $10 \div 25$ deg [15], though greater inclination up to 75 deg does appear, too. If a machined surface is defined as a portion of a cylinder of axis y and radius R , such setting enables us to combine planar/cylindrical surfaces, as in e.g. [16], while ramping and contouring strategies are applied in preference. However, the testing part may consist of quite different surfaces, such as e.g. surfaces which are smooth and dragged, and hemispheric ones [7].

This contribution deals with the investigation of surface roughness based on the calculation of true cusp height Ch while tested part consists of cylindrical surface with defined rounding. It is commonly known, e.g. from [6], that the dimension of the ball end milling cutter is often limited by the part geometry, and the theoretical surface roughness can only be minimized by decreasing the step-over distance a_c [mm]. On the other hand, the tool path needs not be a straight line, as for instance in "ramping" or in "contouring" strategies. If any element is taken off from the free form surface, it consists of an inclined part, the former allows us to model free form surface formation as end milling cutter motion with different directions A in finishing of the free form surface.

3 Geometrical Interpretation of Cusp Height

Let us consider a planar surface from Fig. 2a with inclination angle α_1 to its base. If the ball milling cutter moves along an inclined surface of a workpiece, the effective diameter of the tool leaves tool edge impressions on the newly machined surface. The tool edge impression consists of two elements: one is the cusp bottom line left by the axis of tool rotation and the other is the true cusp height (Ch) due to radial step-over a_e [mm], a factor resulting from machine tool programming. From the point of view of machining, an end ball milling cutter of effective diameter D_e removes axial depth of cut a_p [mm]

If α_1 equals to zero, the plain surface resulting from removal of a_p achieves theoretical cusp height Ch as:

$$\text{Ch} = \frac{D_e}{2} - \sqrt{\left(\frac{D_e}{2}\right)^2 - \left(\frac{a_e}{2}\right)^2} \quad (1)$$

If angle $\alpha_1 \neq 0$, and obviously $\alpha_1 > 0$, the theoretical cusp height depends on α_1 as:

$$\text{Ch} = \frac{D_e}{2} - \sqrt{\left(\frac{D_e}{2}\right)^2 - \left(\frac{a_e}{2 \cdot \cos \alpha_1}\right)^2} \quad (2)$$

Let us consider the cusp bottom line shown in Fig. 2b, an inclined elementary surface. Any point at cusp bottom line from Fig. 2b includes the normal unit vector \mathbf{N} expressing the relationship of the cusp bottom line to the tool axis. The inclination angle α_1 has respect to triangle ECD whereas ED is another cusp bottom line. The motion of the tool axis along line DE refers to removal by "ramping", and that means the direction of milling $A = 90$ deg. The triangle BDE includes line BD, which has respect to removal by "contouring" and that assumes step-over a_e being perpendicular to BD, i.e., $A = 0$ deg. Variable direction of motion for ball end milling cutter can be found within $A = 0 \div 90$ deg, and therefore, the true cusp height must differ from those of Equations (1) and (2) because of vector \mathbf{N} . Thus, the actual inclination angle results from angle A as a simple ratio:

$$\text{tg } \alpha_3 = \overline{CE} / \overline{CF} \quad (3)$$

or

$$\alpha_3 = \text{arctg} [\sin A \cdot \text{tg } \alpha_1] \quad (4)$$

while

$$\overline{CD} = \overline{CE} \cdot \text{tg } \alpha_1 \quad (5)$$

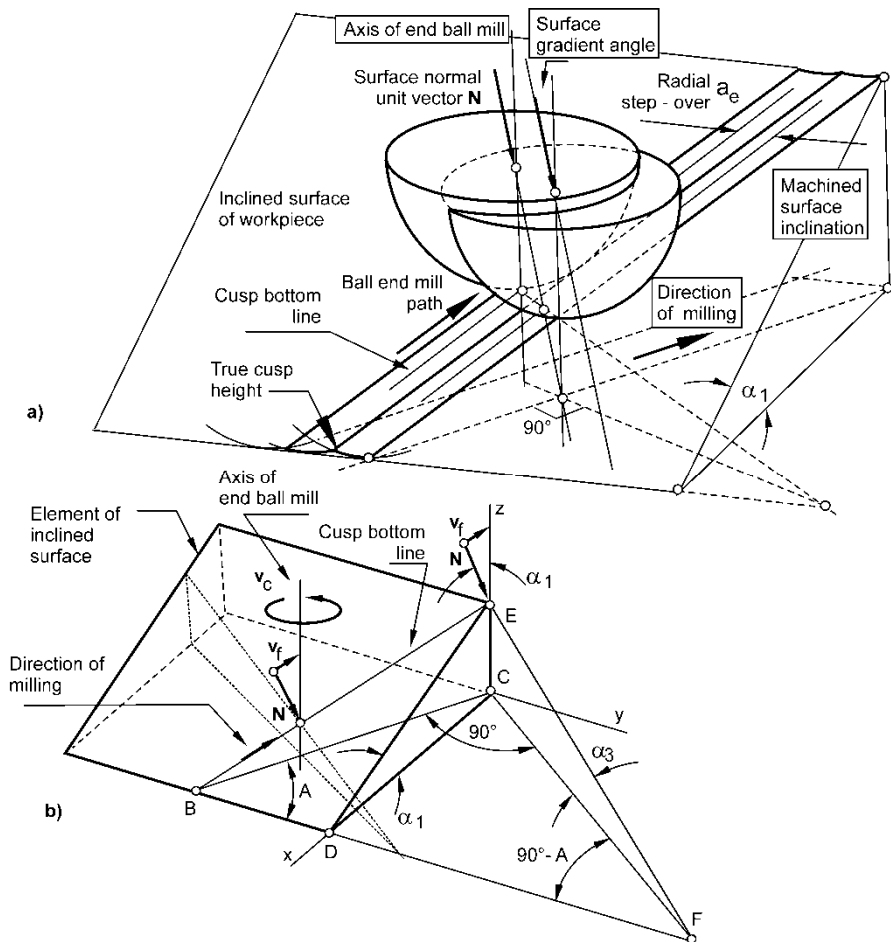


Figure 2

Geometrical interpretation of cusp formation: a) inclined surface with common direction of milling motion; b) element of inclined surface with cusp bottom line as the way of expressing true cusp height and

$$\overline{CF} = \frac{\overline{CE}}{\sin A \cdot \text{tg } \alpha_1} \tag{6}$$

Thus, combining Equations (2) with those of (3) ÷ (6), the true cusp height depending on angle A will be as follows:

$$\text{Ch} = \frac{D_e}{2} - \sqrt{\left(\frac{D_e}{2}\right)^2 - \left(\frac{a_e}{2 \cdot \cos \alpha_3}\right)^2} \tag{7}$$

Let us consider the boundary cases of using Equation (7). If $A = 90^\circ$, or milling of elementary surface in "ramping" strategy of milling, the cusp height does not depend on the vector N . If $A = 0^\circ$, the angle α_3 depends on the roundness of the machined surface, i.e. cusp height Ch depends on the actual angle α_3 derived from α_1 . If $A = 45^\circ$, the true angle $\alpha_3 = \alpha_1$; the latter, however, is not identical with that of from as shown in Fig. 2a. In this case, the true cusp height is not constant.

4 Experimental Study and Process Window Approach

The scope of our experimental research was to determine the effect of the variables in 3D milling on surface roughness data as well as to compare the results with the calculation of true cusp heights according to Equation (7). The tested parts of dimensions 175 x 165 x 45 mm have been designed in such a way that enabled pre-machining of cylindrical semi surfaces with 100 mm surface rounding. It is shown in Fig. 3.

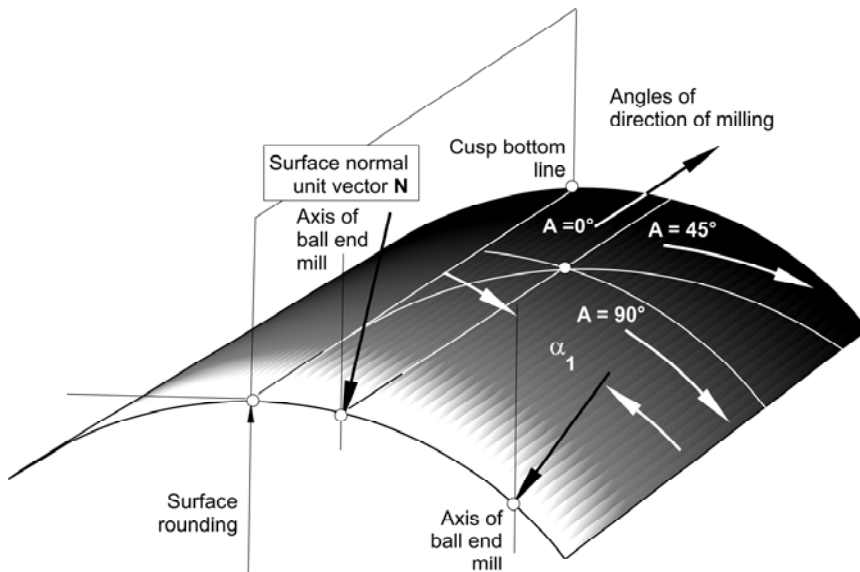


Figure 3

Designed semi-cylindrical surface for experimental research of surface roughness and true cusp height

The semi-cylindrical surface was made from 42CrMo4 steel (1.7225) by rough milling, leaving an allowance of $a_p = 0.2$ mm for surface finishing. Ball end milling cutters of diameter $D = 12$ mm with number of edges $z = 2$ (Fraisa U5286.501) were chosen for the surface finishing. The needed CNC programming was done by Pro/Engineer WF4 CAM and experimental work were conducted by

Mazak Nexus 410A-II machining centre. The surface roughness data were measured with a Mitutoyo Surftest SJ-301 machine.

The first step of exploring the true cusp height was to calculate Ch by the normal vector angle α_1 and milling direction A. Three steps-over, $a_e = 0.20, 0.50,$ and 0.80 mm, as well as three angles, $A = 0^\circ, 45^\circ$ and 90° , in Fig. 3 have been chosen at the outset for cusp height's not depending on cutting conditions. Of cutting conditions, the feed rate v_f [mm/min] is the most influencing quantity for involving feed per tooth f_z [mm] and spindle revolutions n [1/min], and that are factors being set by the machine tool. Thus, three feed rates ($v_f = 630; 950$ and 1265 [mm/min]) have been used. Thus, the applicable space of exploring quantities is shown in Fig. 4, assuming angles α_1 and α_3 are constant.

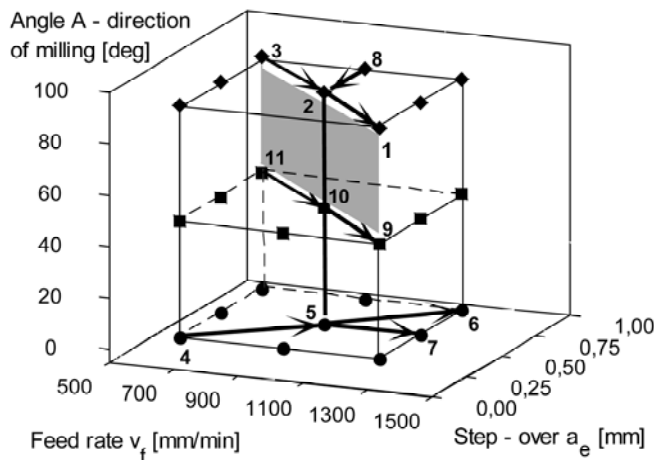


Figure 4

Applicable space of exploring quantities applied to experimental research

Roundness of machined semi-cylindrical surface by Fig. 3 have been prepared in such a way as to enable variation of angle α_1 within $0 \div 45^\circ$. Five values of angle α_1 from Fig. 5 have been used in experimental works for covering completely roundness of machined of only half of semi-cylindrical surface.

Fig. 4 implies that the space of three variables $v_f - a_e - A$ gives $N = 3^3$ measuring points, which correspond to the only value of angle α_1 . If all angles α_1 are assumed to be included into the aim of work, the whole number of measurement would have been equal to $N = 185$, providing that replication of measuring equals to number one. Therefore, an approach based on process windows has been used to test true cusp height, which combines part of applicable space from Fig. 4 with proper arrangement of measuring shown in Fig. 5.

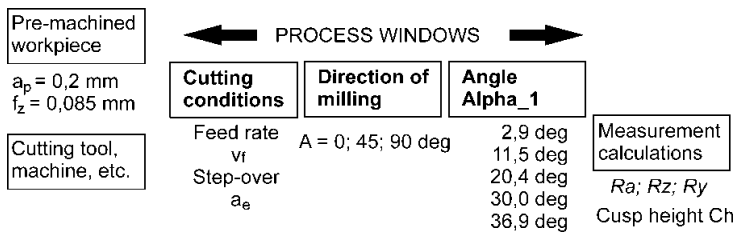


Figure 5

Basic arrangement of influencing quantities producing process windows

Applicable space of exploring quantities in Fig. 4 may be divided into three levels, while $A = 45 \text{ deg}$ produces a boundary between two strategies from Fig. 3, i.e. "ramping" strategy wherein $A = 90 \text{ deg}$ ($\alpha_3 = 0$) and "contouring" strategy with $A = 0 \text{ deg}$ ($\alpha_3 = 2.9, 11.5, 20.4, 30, 36.9 \text{ deg}$). It must be noted that $A = 45 \text{ deg}$ gives $\alpha_3 = 2.05, 8.19, 14.73, 22.21$ and 27.96 deg . In order to reduce the great number of measurements, three windows express the relationship between variables and measured (or calculated) data, while the numbers in Fig. 4 label the measuring points:

- axis of space in Fig. 4, which is created by line 5 – 10 – 2
- panel of space in Fig. 4, which is created by line 1 – 3 – 9 – 11
- diagonals at the bottom/top rectangles complemented by single checking point.

The purpose of windows taken off from space of exploring is to explore the relationships as well as proper comparisons. The former and the latter are very suitable tools for choosing a proper machining strategy for expressing circumstances where undesirable cusp heights appear and thus contribute to the reduction of additional finishing operations when 3D milling.

5 Evaluation Results

Overall results include measured data (roughness average Ra , average maximum height of profile Rz , maximum height of profile Ry) and calculated values of Ch. The former can be reviewed either as qualitative understanding or as any form of dependence. Quantitative understanding means two ways of data expressing. The first is the combination of angles A , α_1 and α_3 and determines the surface without needing additional finishing. Three points in Fig. 4 (i.e., 1, 4 and 10), all of them performing metal removal with $a_c = 0.2 \text{ mm}$, produce roughness Ra no greater than $1.50 \mu\text{m}$, a condition where there is no need to apply additional surface finishing, see in [5]. However, such a condition must be accompanied with further data as shown in Tab. 2. It is obvious that there is no uniformity in ranging of the further roughness data and calculated cusp Ch does not fit with measured Ry either. All cases in Tab. 2 return Ch within a range $0.83 \div 1.30 \mu\text{m}$, i.e. $Ry \gg Ch$.

On the other hand, the unacceptable cases as two points 6 and 8 have been found out in Fig. 4, where measured $R_y > 20 \mu\text{m}$, and $\text{Ch} = 13.35 \div 20 \mu\text{m}$. Finally, point 11 in Fig. 4 is the only case wherein measured R_y ($13.32 \div 19.35 \mu\text{m}$) approaches in very way to the calculated Ch ($13.37 \div 17.12 \mu\text{m}$).

Table 2

The ranges of the best roughness data depending on milling direction

$A = 90^\circ; v_f = 1265 \text{ m/min}$	$A = 0^\circ; v_f = 630 \text{ m/min}$	$A = 45^\circ; v_f = 1265 \text{ m/min}$
$Ra = 0.53 \div 0.93 \mu\text{m}$	$Ra = 0.62 \div 1.22 \mu\text{m}$	$Ra = 0.67 \div 1.25 \mu\text{m}$
$Rz = 2.48 \div 3.45 \mu\text{m}$	$Rz = 4.03 \div 6.22 \mu\text{m}$	$Rz = 3.42 \div 6.33 \mu\text{m}$
$Ry = 2.77 \div 4.05 \mu\text{m}$	$Ry = 6.52 \div 11.05 \mu\text{m}$	$Ry = 3.96 \div 8.25 \mu\text{m}$

Axis of the explored space, line 5 – 10 – 2 gives a way of expressing the relationship between the surface data, and hence can be considered as the one of various process windows. The measurement of machined surface leads to the well-known Ra vs. Rz relationship which characterizes either machining process (e.g. turning, etc.), or applied tool material [17]. If the position of the edge of a rounded ball end mill depends on normal angles α_1 and α_3 , angle of milling direction A has two definite consequences see in Fig. 6.

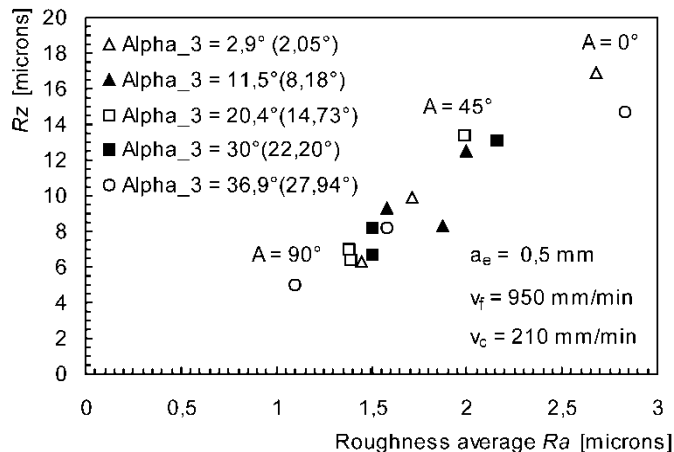


Figure 6

Relationship between Ra and Rz when milling surface with definite roundness (angle α_3 in parentheses are valid for $A = 45 \text{ deg}$ only)

The first consequence of the above is that the relationships in Fig. 6 are expressible in such a way as those in common theory of machining, though the dividing line is given by angle A . Considering angle α_3 , another consequence is that the greater α_3 is the better the final roughness occurs without appearing tool edge marks. Concerning Ra , data resulting from $A = 90^\circ$ draw on results from [3] and [4] but data Rz are comparable with those from [8].

Panel 1 – 3 – 9 – 11 in Fig. 4 displays another process window which is treated particularly as a comparison. Let us follow the line 1 – 9 expressing the influence of direction of milling on cusp height A on both R_y and Ch . While calculation of Ch gives results of order 10^{-1} , the measured roughness – irrespective of R_z or R_y – appears in or of 10^0 as shown in Fig. 7.

Another fact is that the removal by "ramping" strategy of milling ($A = 90$ deg) is not affected by angle α_3 , i.e. the maximum height of the profile holds roughly constant. If the direction of milling is $A = 45^\circ$, the resultant maximum height of profile R_y is strongly reduced by the angle $\alpha_3 = \alpha_1$. Nevertheless, it can be seen that there is a very different variation span of roughness in terms of values R_y . The greater angle α_3 , as a rule, reduces R_y due to true contact between rounded tool edges of ball end mill cutter. However, the distortion of resultant roughness results from marks of the cutter left on the machined surface [18].

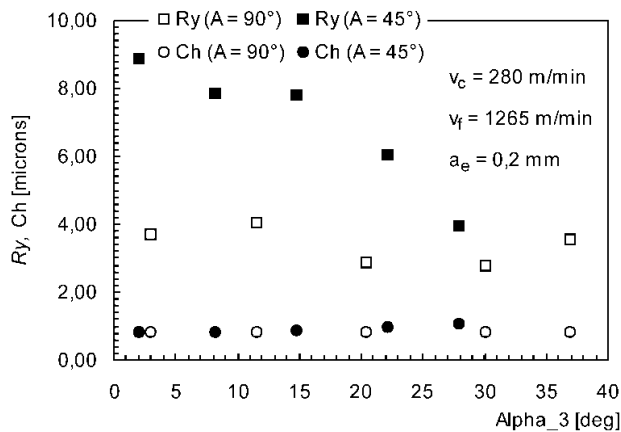


Figure 7

Process window as effect of angle α_3 on maximum height of the profile R_y and its comparison with calculated cusp height Ch

Fig. 8 shows the overall panel 1 – 3 – 9 – 11, and that is the process window expressing spans of roughness R ; the latter depends on both angles α_3 and A . There are two points: 3 (thick line) and 11 (bold line) in Fig. 8 wherein measured R_y values roughly approach the calculated cusp height Ch . However, the wide span of measured R_y from point 3 results rather from a small cutting speed. It is obvious that the increase of feed rate (and cutting speed) brings about a reduction of span of measured R_y data if $A = 90$ deg, whereas calculated Ch is far from the measured R_y in such case. Nevertheless, the variation of angle α_3 along the surface with definite roundness shows quite different effects when the direction of tool motion is equal to $A = 45^\circ$. As indicated by bold lines in Fig. 8, there is perhaps a reversal progress of spans in the measurement of R_y : the greater the feed rate, the greater are the spans of the measured roughness values R_y .

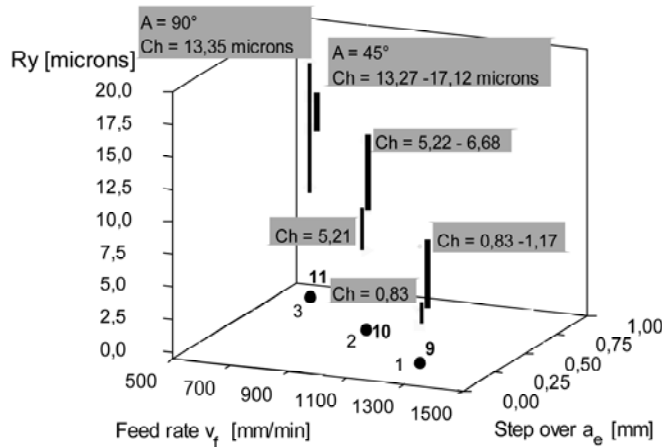


Figure 8

Spans of measured R_y and their comparison with calculated cusp height Ch

Figs. 9a and 9b introduce a way of reducing cusp height due to angle α_3 , the variable appearing in the calculation of Ch . In the case of $A = 90$ deg from Fig. 9a, the chosen angles α_3 of overall process window 1 – 3 – 9 – 11 give the sequence of how tool edge marks merge into resultant tool edge footprint producing desired roughness R_a . The results from $A = 45^\circ$ shown in Fig. 9a give a similar sequence, yet yield better data of R_a without evidence of tool edge marks for point No. 9 of process window 1 – 3 – 9 – 11. On the other hand, the disappearance of tool edge marks due to angle α_3 means no direct improvement in the quality of the machined surface as shown in Fig. 9b. The resultant roughness still depends on step-over a_e , and in such case the calculated Ch fits well to measured roughness values R_y .

6 Discussion and Outlook

The bottom panel of exploring space, or points 3 – 4 – 5 – 6 – 7 with $A = 0^\circ$ give very poor correlation with the calculated value of Ch with measured values of R_y . Nevertheless, the smallest feed rate gives the best results of R_a shown in Tab. 2. There is always a possibility to reduce resultant R_a by increasing the feed rate up to 1265 m/min; however, step-over must be held constant in such a case. Once the proper agreement of Ch with measured R_y has been discovered, when A equals to 45 deg, a point 11 of exploring space. Such a result, however, can be expected when the smallest step-over a_e is used. The angle $A = 90$ gives an approach Ch to measured R_y twice for Ch not being affected by angle α_3 in such case. There is only the highest feed rate which avoids appearance of undesired cusp height Ch , see e.g. data from Tab. 2.

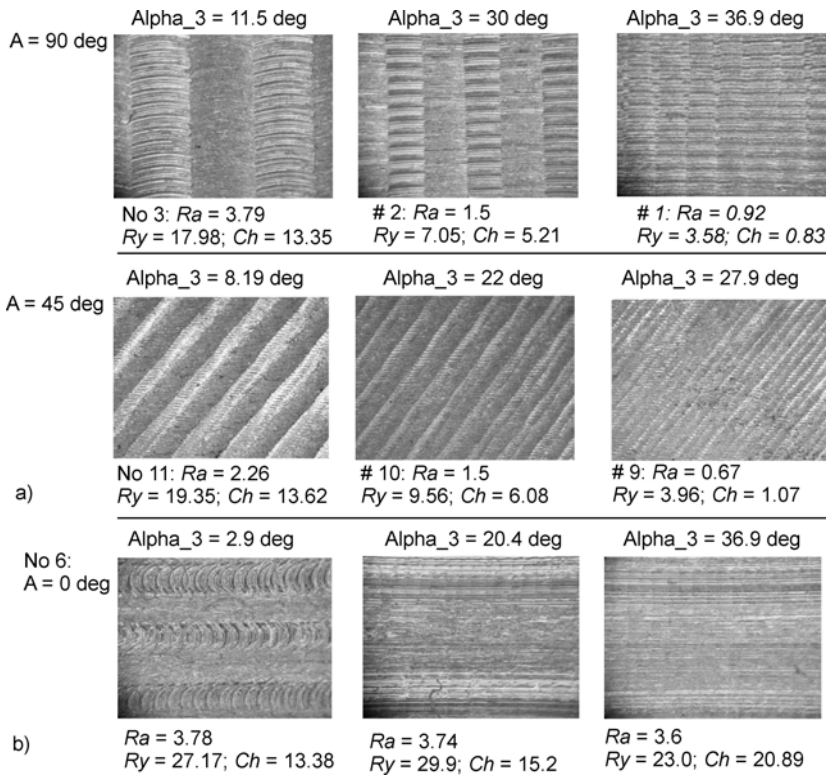


Figure 9

Effect of cutting conditions (feed rate v_f and step – over a_e) on resultant surface texture being affected by angle α_3 : a) process window from panel 1 – 3 – 9 – 11 from exploring space; b) surface texture in point 6 of exploring space as a fragment of bottom process window (all roughness data in microns)

Broadly speaking, an arbitrary strategy of removal by Fig. 3 enables us to obtain a desired roughness that avoids further finishing operations; however, there are roughness variations for angle α_3 changed progressively. Thus, not only does the measured roughness value characterize the machined surface of definite rounding. An option is to indicate true results Ra , Rz , Ry , etc., for instance, $Ra = 0.61/30^\circ$, $Ry/25^\circ$, and so on. Another option is to display the results as spans in terms of Fig. 8. However, the surface normal vectors must be accompanied with measured roughness values as shown in Fig. 6.

An examination of about sixty microscopic photo shots of surface texture, as well as the examination of measured data, showed that the achieved results conform well to data presented in Tab. 1. For instance, the measured results $Rz = 2.50 \div 3.22$ from upper panel of exploring space (point No. 1 in Fig. 4) match well to results from [8], where obtained data are based on the milling of an oblique surface. As far as roughness average in molding and tool making, the best Ra data obtained never exceeded those from [4].

Because of the wide flexibility of designed free form surface, measured roughness represents only one criterion of product quality. Thus, further research will aim to examine mechanisms that accompany the formation of free form surface due to the variability of cutting forces. Surface formation and related forces shall contribute to explain formation of precision of any free form surfaces. The initial steps were carried out and presented in [18].

Conclusions

Strategies chosen when machining free-form surfaces affect the resulting quality of the final product as well as cost per piece. Suitable combinations of strategies reduce total machining time, and do influence the surface quality of the free form surface. Thus, based on achieved experimental results, the following conclusions can be drawn.

- Considerable effects of surface normal vector on resultant roughness produced by ball end milling tool have been found. The greater the leading angle of surface normal, the better the surface finish with definite roundness.
- The desired surface quality results from merging tool edge marks into continuous surface based on the tool footprint because of suppressing cusp height. Such effect is accomplished by combinations between cutting conditions (a_e , v_f) and vector N .
- Evaluation by the Process Window Approach showed that there are diverse effects of angle A , direction of milling surface with defined rounding. Reversal progress of roughness of R_y spans was proved when applying the angles $A = 45$ and $A = 90$ deg.
- Calculated cusp height Ch approaches exceptionally to the measured roughness R_y because of the surface formation's mechanisms in front of the tool edges. An improvement in surface finish appears due to merging of tool edge marks.

Acknowledgement

Research works have been supported by Agency of Research and Development APPV, under contracts No DO7RP-0014-09 and contracts of Bilateral cooperation Slovakia – Hungary SK-HU 0015-08 IMPRICAM. The Slovak authors express their thanks for projects VEGA 1/0500/12 “Quality improvement when milling form surfaces by advanced milling tools” and VEGA No. 1/0279/11 “Integration of trials numerical simulation and neural network to predict cutting tool performance”, supported by Scientific Grant Agency of the Ministry of Education, Science and Research of Slovakia.

The project was realized through the assistance of the European Union, with the co-financing of the European Social Fund: TÁMOP-4.2.1.B-11/2/KMR-2011-0001 Researches on Critical Infrastructure Protection.

References

- [1] Byrne G. et al. Advancing Cutting Technology, *Annals of the CIRP*, 52 (2003) 2, 483-507
- [2] Taylan A et al.: Manufacturing of Dies and Molds. *CIRP Annals – Manufacturing Technology Volume 50*, 2 (2001) pp. 404-422
- [3] Gilles P. et al: Dynamic Behaviour Improvement for a Torus Milling Cutter using Balance of the Transversal Cutting Force. *Int J Adv Manuf Technol* (2009) 40:669-675
- [4] Becze, C. E. et al.: High-Speed Five-Axis Milling of Hardened Tool Steel *International Journal of Machine Tools & Manufacture* 40 (2000) 869-885
- [5] Baptista, R, Antune Simoes, J. F.: Three and Five Axes Milling of Sculptured Surfaces. *Journal of Materials Processing Technology* 103 (2000) 398-403
- [6] Fallböhmer, P. et al.: High-Speed Machining of Cast Iron and Alloy Steels for Die and Mold Manufacturing. *Journal of Materials Processing Technology* 98 (2000) 104-115
- [7] Lopez de Lacalle L. N. et al.: Toolpath Selection Based on the Minimum Deflection Cutting Forces in the Programming of Complex surfaces Milling. *International Journal of Machine Tools & Manufacture* 47 (2007) 388-400
- [8] Antoniadis A. et al.: Prediction of Surface Topomorphy and Roughness in Ball-End Milling. *Int J Adv Manuf Technol* (2003) 21:965-971
- [9] Lartigue, C. et al.: CNC Tool Path in Terms of B-Spline Curves. *Computer-aided Design* 33 (2001) 307-319
- [10] Warkentin, A. et al.: Comparison between Multi-Point and Other 5-Axis Tool Positioning Strategies. *International Journal of Machine Tools & Manufacture* 40 (2000) 185-208
- [11] Jerard, R. et al.: Methods for Detecting Errors in Numerically Controlled Machining of Sculptured Surfaces. *IEEE Computer Graphics & Applications*, 10 (1989) 1, 26-39
- [12] Narita H. et al.: Trial-Less Using Virtual Machining Simulator for Ball End Milling Operations. *JSME International Journal Series C*, 49 (2006) 1, 50-55
- [13] Ozturk B. et al.: Machining of Free-Form Surfaces. Part II: Calibration and Forces. *International Journal of Machine Tools & Manufacture* 46 (2006) 736-746
- [14] Date H. et al.: Wavelet-based Multiresolution Representation of a Geometric Model for Free-Form Surface Machining. *Proc. of the 2000*

- Japan–USA Flexible Automation Conf., July 23–26, 2000, Ann Arbor, Michigan, 2000JUSFA–13035, pp 1–8
- [15] Imani, B. M. et al.: An Improved Process Simulation System for Ball-End Milling of Sculptured Surfaces. *International Journal of Machine Tools & Manufacture* 38 (1998) 1089–1107
- [16] Kim G. M. et al.: Cutting Force Prediction of Sculptured Surface Ball-End Milling Using Z-Map. *International Journal of Machine Tools & Manufacture* 40 (2000) 277–291
- [17] Beňo, J.: *Theory of Innovative Technology*. Viena Kosice (2010) 175, pp. (in Slovak language)
- [18] Ižol P., Beňo J., Mikó B.: Precision and Surface Roughness when Free Form Milling. *Manufacturing Engineering*, 10 (2011) 1, pp. 70–73